V_2O_5/TiO_2 Catalyst Xerogels: Method of Preparation and Characterization

CRISTIANE B. RODELLA, ROBERTO W.A. FRANCO, CLAUDIO J. MAGON,
JOSE P. DONOSO AND LUIS A.O. NUNES
Instituto de Física de São Carlos, USP, C.P. 369, CEP: 13560-970, São Carlos, SP, Brazil

MARGARIDA J. SAEKI
Departamento de Química, FC, UNESP, C.P. 473, CEP: 17033-360, Bauru, SP, Brazil

MICHEL A. AEGERTER
Institut für Neue Materialien, 66123, Saarbrücken, Germany

ARIOVALDO O. FLORENTINO*
Departamento de Química e Bioquímica, IB, UNESP, C.P. 510, CEP: 18618-000, Botucatu, SP, Brazil
arif@ibb.unesp.br

Received December 8, 2000; Accepted March 6, 2002

Abstract. This work describes a modified sol-gel method for the preparation of V_2O_5/TiO_2 catalysts. The samples have been characterized by N_2 adsorption at 77 K, X-ray Diffractometry (XRD), Scanning Electronic Microscopy (SEM/EDX) and Fourier Transform Infrared Spectroscopy (FT-IR). The surface area increases with the vanadia loading from 24 $m^2\ g^{-1}$ for pure TiO_2 to 87 $m^2\ g^{-1}$ for 9 wt% of V_2O_5. The rutile form is predominant for pure TiO_2 but becomes enriched with anatase phase when vanadia loading is increased. No crystalline V_2O_5 phase was observed in the diffractograms of the catalysts. Analysis by SEM showed heterogeneous granulation of particles with high vanadium dispersion. Two species of surface vanadium were observed by FT-IR spectroscopy: a monomeric vanadyl and polymeric vanadates. The vanadyl/vanadate ratio remains practically constant. Ethanol oxidation was used as a catalytic test in a temperature range from 350 to 560 K. The catalytic activity starts around 380 K. For the sample with 9 wt% of vanadia, the conversion of ethanol into acetaldehyde as the main product was approximately 90% at 473 K.

Keywords: sol-gel, vanadium and titanium oxide, catalyst, ethanol oxidation

1. Introduction

Vanadia supported on titania, V_2O_5/TiO_2, constitutes a well-known catalytic system for selective oxidation [1–4] and ammoxidation of hydrocarbons [2, 5] as well as selective reduction of NO_x with NH_3 in the presence of O_2 [6–9]. Some works have shown that a higher activity and selectivity for both applications is achieved when vanadia is supported on anatase, rather than rutile TiO_2 [8–14]. Many hypotheses have been reported to explain this synergistic effect of anatase as a support in V_2O_5/TiO_2 catalysts. Vejux and Courtine [15] have proposed that a close epitaxial crystallographic match between the structure of the (010) plane of V_2O_5 and the (001) plane of anatase leads to the spreading and preferential exposure of the (010) active crystalline plane.

*To whom all correspondence should be addressed.

Bond [14] considered the formation of a stable VO_x monolayer over anatase TiO_2 and similar electronegativities of titanium and vanadium as the main reasons for the apparent superior catalytic performance. As a consequence, anatase has been employed as a support or as a component in a number of commercially important heterogeneous catalyst systems [16, 17]. In spite of this advantage, titania, as a support, prepared by conventional ceramic processes, suffers from limited surface area, lack of abrasion resistance, poor mechanical strength, and high price. In addition, the anatase phase has poor thermal stability at high temperature [18]. Temperature stability in catalysis is vitally important, since, in high temperature oxidations, long-term thermal stability dictates the catalyst life. Its partial transformation into rutile is thermodynamically favored but leads to a worsening of catalytic performance. This occurs as a consequence of a decrease in surface area and destruction of the active monolayer of vanadia spread over the anatase surface. Because of these reasons, a mixed titanium oxide support has been preferred over a single titanium oxide support.

The stabilization of the active phase in vanadia/titania systems depends mainly on the characteristics of the support and of the preparation methods. Currently, efforts are being made to develop new oxide supports to satisfy the needs of practical applications [18, 19].

The sol-gel method has been proposed as an alternative to synthesize catalysts with a high surface area and stable active phase [20–23]. Several procedures have been proposed: co-gelling of vanadia and titania [21, 22], preparation of aerogels by two-step procedure [24], impregnation of V_2O_5 on TiO_2 aerogels [8, 9] and hydrogels [25]. In all these studies, V_2O_5 was either immobilized on pre-formed anatase or vanadium and titanium oxides were allowed to gel by a procedure that favors the anatase formation. The role of the active phase in the modification of the textural and structural properties of the support, and hence in the active phase itself, has received little attention.

The present work focuses on the preparation of V_2O_5/TiO_2 catalysts using a modified sol-gel method to obtain a support with highly dispersed V^{4+} and V^{5+} ions. Physico-chemical characterization of the materials were carried out by N_2 adsorption at 77 K (BET), X-ray Diffractometry (XRD), Scanning Electronic Microscopy (SEM/EDX) and Infrared Spectroscopy (FT-IR). A preliminary catalytic test was performed for the ethanol oxidation in the temperature range from 350 K to 560 K.

2. Experimental

2.1. Sample Preparation

V_2O_5/TiO_2 catalysts with different contents of V_2O_5 were synthesized by using a modification of the sol-gel method reported in [22, 23]. The preparation procedure is shown schematically in Fig. 1. All reagents were used without further purification. Solution (A) was prepared by dissolving desired amounts of ammonium metavanadate (Carlo Erba 99.5%) in an aqueous solution (pH = 1.0) of nitric acid (Merck p.a.) and subjected to ultrasonic vibration at 75 W for 1 minute. Solution (B) was prepared by diluting tetraisopropyl orthotitanate (Fluka 99.9%) in isopropyl alcohol (Merck 99.7%) with molar ratio of 0.25:1.0. Then, solution (A) was added to solution (B) and a gel was immediately formed (pH = 1.0). The gel was vigorously stirred for 5 min under ultrasonic vibration at 75 W and maintained at rest at room temperature. After 24 h, the resulting gel was dried at 373 K for 4 h, then heated to 723 K in air, at a heating rate of 5 K min^{-1}, and calcined at 723 K for 16 h. The catalysts obtained

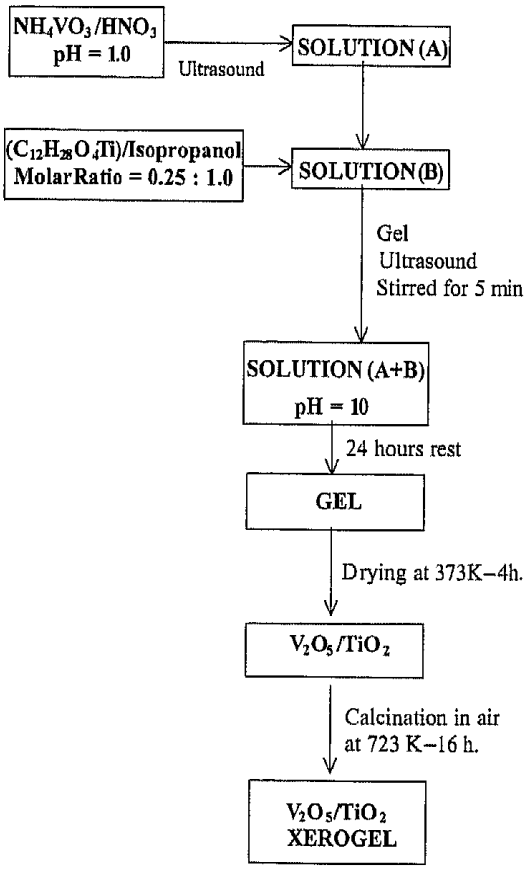

Figure 1. Preparation scheme of the V_2O_5/TiO_2 catalysts by modified sol-gel method.

were: 3, 6 and 9% V_2O_5/TiO_2. Pure TiO_2 was prepared also.

2.2. *Sample Characterization*

Surface areas were determined using the BET method using a Micromeritics model AccuSorb 2100E instrument. X-ray diffractometry (powder technique) was carried out with a Rigaku Rotaflex diffractometer model RU 200B, using Cu Kα radiation (nickel filter). The reflections present in the diffractograms of the samples were compared to JPDS powder data files. Particle size and morphology of samples of pure TiO_2, 6, and 9 wt% V_2O_5 were investigated using a Zeiss Scanning Electronic Microscope model DSM 960. Infrared studies of the 3, 6 and 9% V_2O_5/TiO_2 catalysts were performed with a Nicolet FT-IR spectrophotometer model Magma 850 using the photoacoustic detection system MTEC model 300 (resolution 4 cm^{-1}, 5000 scans). The background spectrum of the pure TiO_2 was electronically subtracted from the FT-IR catalysts spectra. To avoid moisture contamination helium (99.996%) was passed through the sample during FT-IR measurements. Prior to acquisitions of FT-IR spectra, samples were first dried overnight in vacuum at 503 K.

2.3. *Catalytic Test*

The conversion of ethanol was tested in a temperature range from 350 K to 560 K with a residence time $W/F = 7.4$ g cat mol h^{-1}, W being the weight of the catalysts (g cat.) and F the total flow of the gases (mol h^{-1}). The molar ratio of the standard reactant (ethanol-oxygen) and the diluting gas (helium) was 1:5:10, respectively. An on-line Shimadzu Gas Chromatograph GC-14B using Suple-Q and Carboxen-1010 Plot capillary columns analyzed all products. The absence of a homogeneous combustion of reactants and products at temperatures up to 623 K was confirmed by using powdered Pyrex glass.

3. Results and Discussion

3.1. *Samples Characterization*

BET surface areas of the samples with different content of vanadia are presented in Fig. 2. A surface area of 24 $m^2\ g^{-1}$ was obtained for pure TiO_2 and the presence of the vanadia increased the surface area. It is known that the presence of the anatase phase leads to material with high surface area [28]. These BET surface area results suggest that the presence of the vanadia promotes the anatase phase formation in the V_2O_5/TiO_2 systems obtained by this modified sol-gel method and calcined at 723 K. The isotherms of N_2 adsorption-desorption at 77 K for pure TiO_2 and catalysts with different contents of vanadia are presented in Fig. 3. According to the IUPAC classification [26, 27] type II isotherm profiles with type H2 hysteresis are observed for all samples. They indicate meso

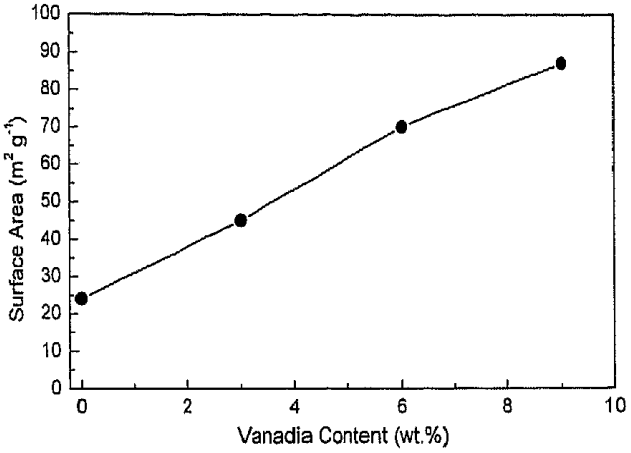

Figure 2. Surface areas of the samples with different content of vanadia.

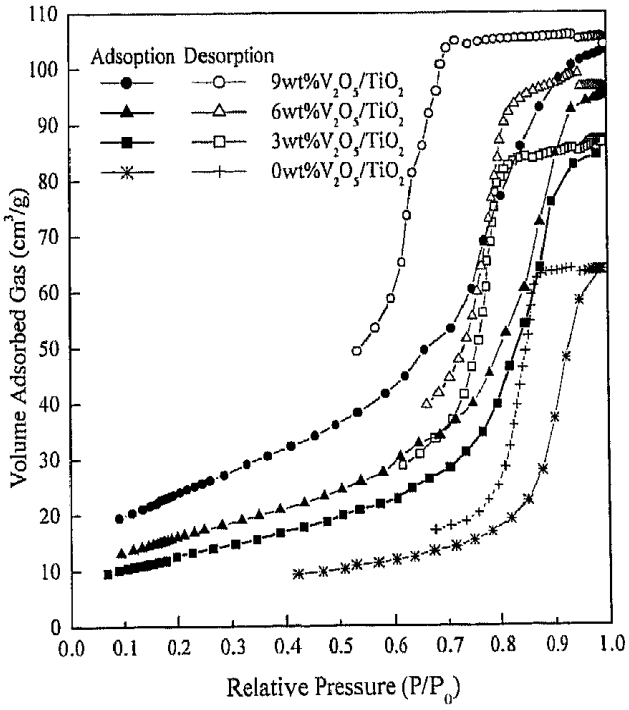

Figure 3. Adsorption/desorption isotherms of N_2 at 77 K of pure TiO_2 and V_2O_5/TiO_2 catalysts. Filled symbols: Adsorption, opens symbols desorption.

($r = 20$–50 Å) and macro ($r > 50$ Å) pores of irregular shapes (slits or bottle shapes). With increasing vanadia content, the adsorption capacity (maximum volume of adsorbed gas by the material at $P/P_0 \cong 1$) increases from 64 cm^3g^{-1} for pure TiO_2, to 105 cm^3g^{-1} for 9 wt% V_2O_5. A qualitative analysis of the adsorption isotherm at low relative pressure [27] shows the presence of micropores ($r < 20$ Å) and an increase of the total volume with the increase of the vanadia content. The average pore diameter decreases from 70 Å for pure TiO_2 to 20 Å for 9 wt% of V_2O_5 (Fig. 4). An almost monomodal pore size distribution is observed for most samples.

Considering the same content of vanadia, the surface areas of the samples obtained here are higher than those obtained by other ceramic preparation methods. Cavani et al. [30] related the preparation of V_2O_5/TiO_2 systems by co-precipitation from an aqueous acidic solution of vanadium and titanium and calcination at 673 K. Samples with content of 10 and 25 wt% of vanadia was obtained with surface area of 68 and 92 m^2g^{-1}, respectively. The modified sol-gel method and the calcination at 723 K proposed yields vanadia/titania catalysts with high surface area [29], with lower content of vanadia, 6 and 9 wt% of V_2O_5, respectively. The titania grain size was calculated by the Scherrer equation for each sample. We observed a trend toward smaller TiO_2 crystallites as vanadium was added: the titania grain size of pure TiO_2 was equal to 62 nm, where the sample with the highest amount of vanadium, it was 25 nm.

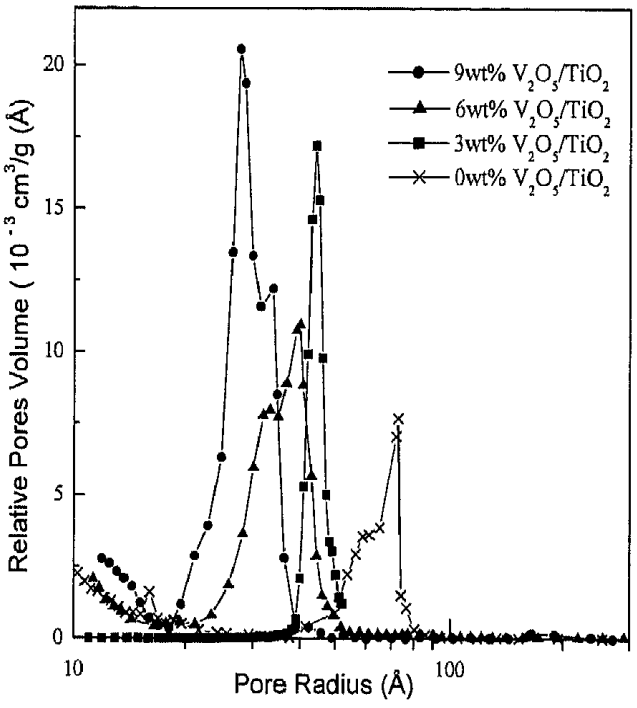

Figure 4. Pore size distribution for pure TiO_2 and V_2O_5/TiO_2 catalysts.

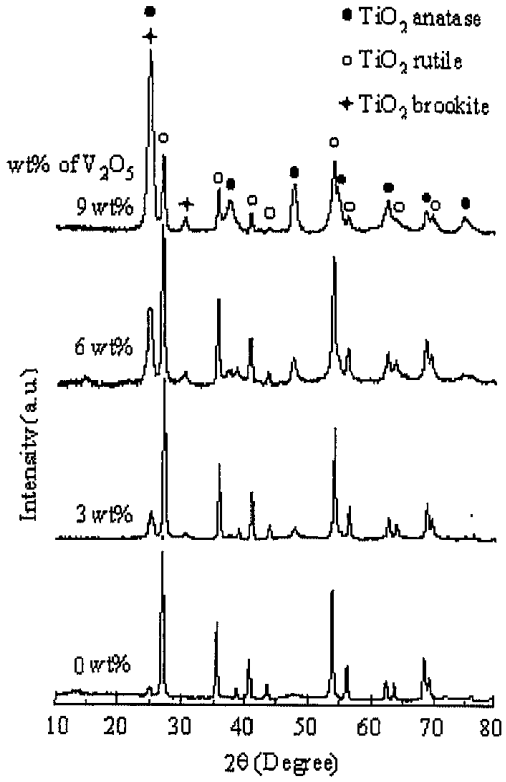

Figure 5. X-ray diffraction patterns of pure TiO_2 and V_2O_5/TiO_2 catalysts.

Figure 5 shows the typical XRD peaks attributed to the anatase, rutile, and brookite phases of the catalysts. Peaks associated with crystalline V_2O_5 are not observed for any samples, indicating the effective distribution of vanadium on the titania matrix. A substantial increase in the anatase peak intensity is observed as the vanadia loading increases. This can be attributed to the strong vanadium-titanium interaction [1], which inhibits the phase transformation of anatase to rutile. Similar effects are related to the presence of impurities, such as sulfate and phosphate, or attributed to a chemical solid interaction between vanadia and anatase [30–33].

The transformation of anatase to rutile is only considered an effective process for TiO_2 samples calcined at temperatures higher than 973 K [30–32, 34]. However, XRD results depicted in Fig. 5 indicate the predominance of rutile for pure TiO_2 calcined at a lower temperature (723 K). This, may be a consequence of a decrease in the phase transition temperature of anatase to rutile promoted by the above preparation method. In acidic preparations, the hydrolysis of the titanium alkoxide is faster than the condensation, producing

samples containing many hydroxyl radicals. The thermal treatment of these samples causes dehydroxylation, and forms$^-$ anionic vacancies [31]. The high defect concentrations of anatase crystals contribute to the decrease in anatase to rutile phase transformation [33]. In short, the structural nature of V_2O_5/TiO_2 is determined by vanadia-titania interactions, being more evident for the V_2O_5/TiO_2 system prepared from liquid precursors [33, 34].

The X-ray diffractogram of the sample with 3 wt% of vanadia show the presence of the anatase phase, but the rutile phase is predominant. With the increase of the vanadium content the peaks of the rutile phase decrease and a substantial increase of the anatase peak intensity is observed. It can be noted that the diffractograms of 6 wt% and 9 wt% V_2O_5 samples show the predominance of the anatase phase. The XRD results show also that even in the 9 wt% vanadia sample, both anatase and rutile forms are present. This is very important, because the vanadia/titania catalysts mechanisms involve redox reactions. Jonson et al. [29] concluded that V^{4+}/V^{5+} couples are more effective than the V^{3+}/V^{4+} pair. However, V^{4+} ions can be reduced to V^{3+} ions in the anatase phase, but cannot be oxized to V^{5+} due to strong interaction between vanadia and titania surface. In the rutile phase the oxidation of V^{4+} to V^{5+} ions occurs, meaning the presence of rutile is required to promote high performance of the catalysts by redox properties.

Figure 6(a)–(c) shows SEM/EDX images of the surface of pure TiO_2, 6 and 9% V_2O_5/TiO_2. The morphology of the pure TiO_2 indicates the formation of

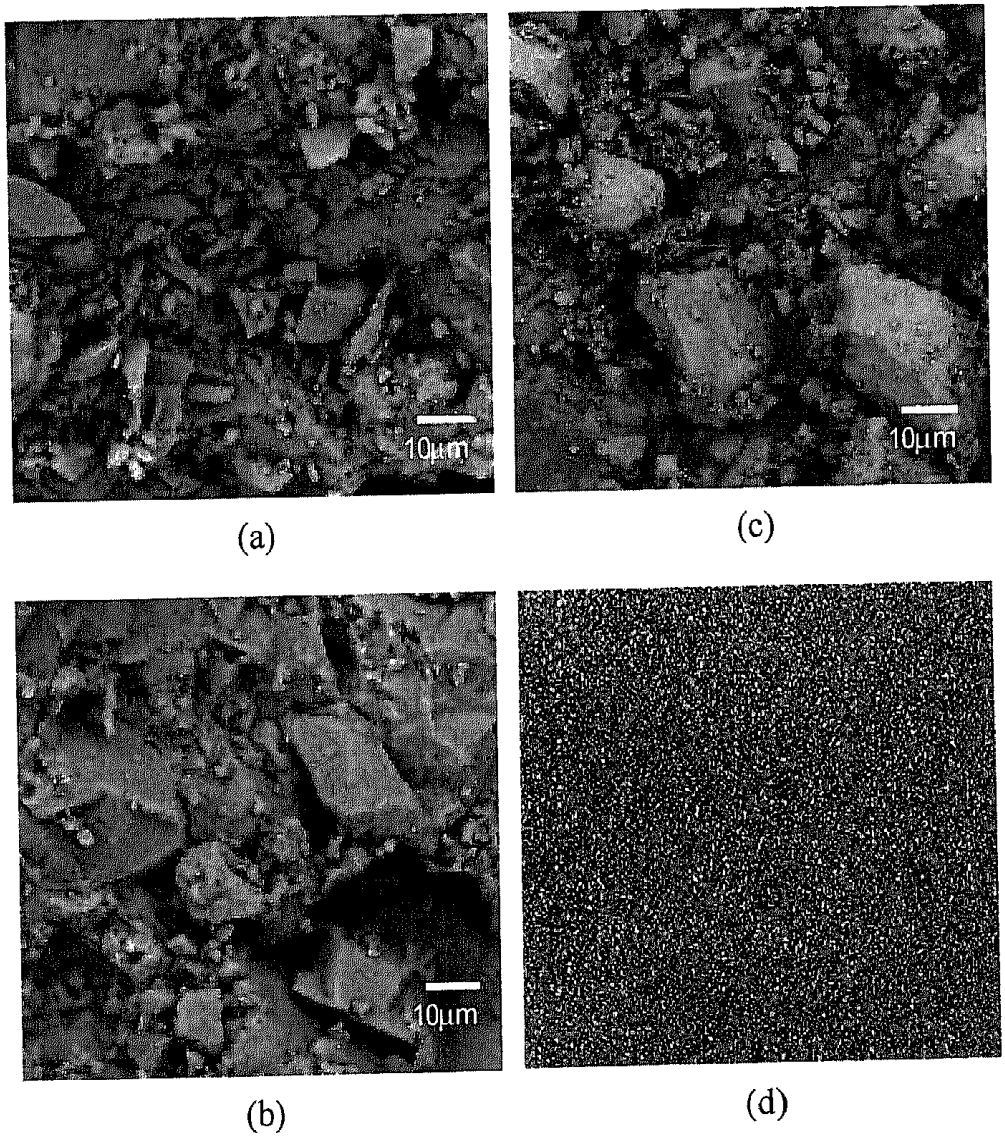

Figure 6. SEM micrographs of V_2O_5/TiO_2 catalysts: (a) TiO_2, (b) 6% V_2O_5/TiO_2, (c) 9% V_2O_5/TiO_2 and (d) EDX dispersive analysis of 9% V_2O_5/TiO_2.

Table 1. EDX analysis of V_2O_5/TiO_2 xerogels.

	EDX analysis (wt%)	
V_2O_5 content (wt%)	V	Ti
0	0	100
3	3.2 ± 0.3	96.7 ± 0.5
6	5.9 ± 0.3	94.2 ± 0.5
9	9.1 ± 0.3	90.8 ± 0.5

agglomerates, with nanoscale particles. There is no significant modification in the morphology with vanadium addition. An EDX analysis of vanadium is shown for the 9% V_2O_5/TiO_2 in Fig. 6(d). Within the sensitivity of the equipment, the analysis indicates a uniform distribution, with no agglomeration of V_2O_5. The results of Table 1 confirm the nominal V/Ti ratios.

Figure 7 shows the FT-IR spectra of V_2O_5/TiO_2 samples recorded between 1300 and 500 cm^{-1} after

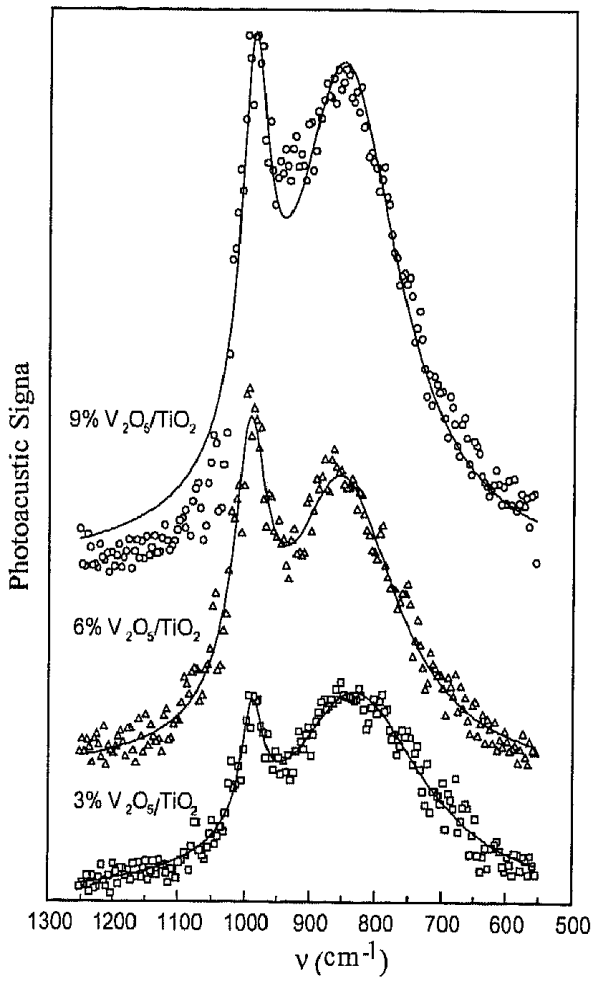

Figure 7. FT-IR spectra of 3, 6 and 9% V_2O_5/TiO_2 dehydrated in vacuum at 503 K for 12 h.

subtraction of the contribution of TiO_2 to the spectra. Two well-defined absorption bands can be seen: one relatively narrow band at 998 cm^{-1} and another broad band spreading from 760 to 940 cm^{-1}. Earlier literature reports a high frequency band, at 1030 cm^{-1}, is associated with surface-isolated vanadyls in water-free samples [35, 36]. Such a band is assigned to the stretching mode of the "monoxo" V=O species, with unsaturated coordination and has the characteristic that its center was shifted to lower energies (995 cm^{-1}) in hydrated samples. This could explain the band observed at 998 cm^{-1}.

The broad absorption band, ranging from 760 to 940 cm^{-1}, is due to different species of vanadates. According to comparable studies, performed with FT-IR and Raman scattering [32], it may correspond to the 920 cm^{-1} Raman band, which is also attributed to the vanadate species. Two vibrational modes have been identified and associated with the O–V–O stretching modes of metavanadate $(VO_3)_n^{n-1}$ species [35]. The low energy mode (870 cm^{-1}) is asymmetric and more easily observed by Raman techniques. Moreover, it has been shown that the infrared spectra of metavanadates do not depend strongly on hydration/dehydration treatments [35]. Figure 7 shows also that the ratio between the intensity of both bands increases with increasing V_2O_5 content but their width and relative intensities remain unchanged. This indicates that the vanadyl/vanadate ratio is independent of the vanadium concentration, and that the two species are homogeneously dispersed on the support surface for samples 3, 6, and 9 wt% of vanadia. Furthermore, the FT-IR spectra of samples do not exhibit band attributed to crystalline V_2O_5, agreeing with the XRD results.

The independence of the vanadyl/vanadate ratio in relation to total vanadium has not been observed in previous studies [34–37], where the vanadyl/vanadate ratio drastically decreases for concentrations higher than 2.5 wt% of vanadia. This modified sol-gel leads to V_2O_5/TiO_2 systems with good distribution of vanadia in the matrix and a tendency to reduce V^{5+} to V^{4+} ions on the support surface. In other words, the increase in vanadia content, increases the anatase phase and promotes a reduction of V^{5+} to V^{4+} proportionally. The anatase phase promotes the reduction of V_2O_5, while rutile phase retards this process. The presence of anatase and rutile phases and V^{5+}/V^{4+} pair are necessary conditions for good performance of the vanadia/

titania systems in oxidation catalysis as discussed below.

3.2. *Catalytic Test*

The activity, after 15 min reaction, of the catalyst as a function of the temperature is shown in Fig. 8. The preliminary results are very promising. The catalysts have already shown some activity at 323 K, which increases with both, vanadia loading and temperature of reaction. The pure TiO_2 exhibits a very low activity for the ethanol oxidation. For the sample with 9 wt% of vanadia, the conversion of ethanol was almost 90% at 450 K. This level was maintained constant during a 5 h run. Acetaldehyde was the main product with acetic acid, ethene, carbon oxides and ethyl acetate as minor products.

The increase of the activity with the increase of the vanadia content can be explained by an increase in the number of active sites. Our data seems to indicate that both, isolated vanadyl and polymeric metavanadate species of vanadium are present. Vanadyl/vanadate ratios stayed almost constant even in the sample with 9 wt% of vanadia. It means that the two species are distributed uniformly on the support surface and such distribution is not affected by vanadium contents even for 9 wt%. Generally, this ratio decreases drastically when the polymerization of the vanadia takes place for samples containing greater than 2.5 wt% of vanadia [25, 37]. Therefore the good performance of our catalysts at lower temperature, especially for 6 and 9 wt% of vanadia, indicate a good distribution of V_2O_5 on the support and the absence of V_2O_5 crystallites.

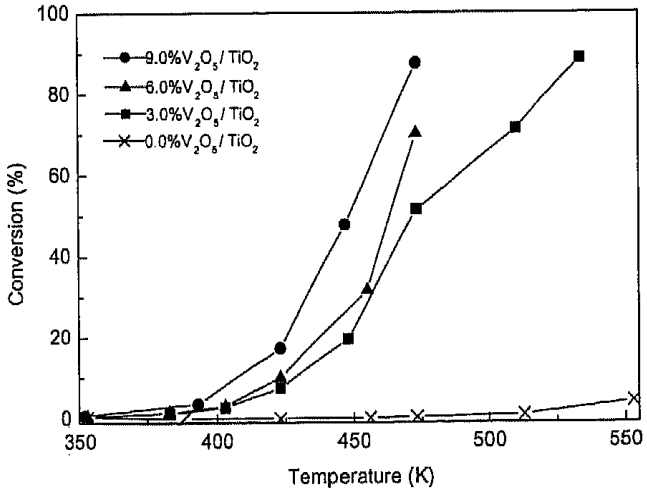

Figure 8. Ethanol oxidation on pure TiO_2 and V_2O_5/TiO_2 catalysts with different loadings of vanadia. Conversion after 15 min of reaction.

4. Conclusions

V_2O_5/TiO_2 catalysts were obtained after calcination at 723 K using sols for which the pH of the precursor solution was controlled ($\approx$1.0), under ultrasonic treatment. This leads to TiO_2 supports containing predominantly the rutile phase. In contrast, the anatase phase is favored by V_2O_5 additions and increases with increasing vanadium concentration. This leads to a V_2O_5/TiO_2 system with heterogeneous granulation of particles and high vanadium dispersion on titania. Additionally, high surface area with meso and macro porosity is achieved at high vanadia loadings. For concentrations above 3 wt%, surface areas are greater than those obtained from samples prepared by conventional ceramic processes. The formation of crystalline V_2O_5 phase was not observed, in any samples. FT-IR spectra identified two species of surface vanadium: monomeric vanadyl and polymeric vanadates. The vanadyl/vanadate ratio remains practically constant indicating that the two species are uniformly distribution on the support. The catalytic activity for ethanol oxidation starts around 380 K. For samples with 9 wt% of vanadia, the conversion was approximately 90% at 473 K, with acetaldehyde as the main product and acetic acid, ethene, carbon oxides and ethyl acetate as minor products.

Acknowledgments

The authors are grateful to the FAPESP, CNPq and FUNDUNESP Foundations (Brazil) for financial support.

References

1. B. Grzybowska-Swierkosz, Appl. Catal. A **157**, 263 (1997).
2. K.V. Narayana, A. Venugopal, K.S. Rama Rao, S. Khaja Masthan, V. Venkat Rao, and P. Kanta Rao, Appl. Catal. A **167**, 11 (1998).
3. C.R. Dias, M.F. Portela, and G.C. Bond, J. Catal. **157**, 344 (1995).
4. T. Mongkhonsi and L. Kershenbaun, Appl. Catal. A **170**, 33 (1998).
5. G. Centi, Appl. Catal. A **147**, 267 (1996).
6. M.D. Amiridis, I.E. Wachs, G. Deo, J.-M. Jehng, and D.S. Kim, J. Catal. **161**, 247 (1996).
7. L. Casagrand, L. Lietti, I. Nova, P. Forzatti, and A. Baiber, Appl. Catal. B **22**, 63 (1999).
8. O. Zegaoui, C. Hoang-Van, and M. Karroua, Appl. Catal. B **9**, 211 (1996).
9. M.A. Reiche, E. Ortelli, and A. Baiker, Appl. Catal. B: Environm. **23**, 187 (1999).

10. G. Centi, E. Giamello, D. Pinelli, and F. Trifirò, J. Catal. **130**, 220 (1991).
11. K.V.R. Chary, G. Kishan, T. Bhaskar, and C.J. Sivaraj, J. Phys. Chem. B **102**, 6792 (1998).
12. P. Courtine and E. Bordes, Appl. Catal. A **157**, 45 (1997).
13. G.C. Bond, Appl. Catal. A **157**, 91 (1997).
14. G.C. Bond, S. Flamerz, and R. Shukri, Faraday Disc. Chem. Soc. **78**, 65 (1989).
15. A. Vejux and P. Courtine, J. Solid State Chem. **23**, 93 (1978).
16. L. Lietti, G. Ramis, F. Berti, G. Toledo, D. Robba, G. Busca, and P. Forzatti, Catal. Today **42**, 101 (1998).
17. G. Busca, M. Baldi, C. Pistarino, J.M.G. Amores, V.S. Escribano, E. Finocchio, G. Romezano, F. Bregan, and G.P. Toledo, Catal. Today **53**, 525 (1999).
18. B.M. Reddy, B. Chowdhurry, I. Ganesh, E.P. Reddy, T.C. Rojas, and A. Fernández, J. Phys. Chem. B **102**, 10178 (1998).
19. G.T. Went, L.-J. Leu, R. Rosin, and A.T. Bell, J. Catal. **134**, 492 (1992).
20. G.M. Pajonk, Appl. Catal. **72**, 217 (1991).
21. M.A. Cauqui and J.M. Rodríguez-Izquierdo, J. Non-Cryst. Solids **147/148**, 724 (1992).
22. M. Schneider, M. Maciejewski, S. Tschudin, A. Wokaun, and A. Baiker, J. Catal. **149**, 326 (1994).
23. J.B. Miller, S.T. Johnston, and E.I. Ko, J. Catal. **150**, 311 (1994).
24. C. Hoang-Van, O. Zegaoui, and P Richat, J. Non-Cryst. Solids **225**, 157 (1998).
25. G. Centi, D. Pinelli, F. Trifiró, D. Ghoussoub, M. Guelton, and L. Gengembre, J. Catal. **130**, 238 (1991).
26. P. Schneider, Appl. Catal. **129**, 157 (1995).
27. S.J. Gregg and K.S.W. Sing, *Adsorption, Surface Area and Porosity* (Academic Press, London, 1982).
28. J.L.G. Fierro, in *Spectroscopic Characterization of Heterogeneous Catalysts—Part A: Methods of Surface Analysis* (Elsevier Science Publishers, Amsterdam, 1990), ch. 3.
29. B. Jonson, B. Rebenstorf, R. Larsson, S. Lars, and T. Andersson, J. Chem. Soc., Faraday Trans. **84**, 3547 (1988).
30. F. Cavani, G. Centi, E. Foresti, F. Trifirò, and G. Busca, J. Chem. Soc., Faraday Trans. **84**, 237 (1988).
31. M. Gasior and T. Machej, J. Catal. **83**, 472 (1983).
32. L. Lietti, P. Forzatti, G. Ramis, G. Busca, and F. Bregani, Appl. Catal. B **3**, 13 (1993).
33. G.T. Went, L.-J. Leu, and A.T. Bell, J. Catal. **134**, 479 (1992).
34. L. Dall'Acqua, M. Baricco, F. Berti, L. Lietti, and E. Giamello, J. Mater. Chem. **8**, 1441 (1998).